Journal of Biomolecular NMR, **14:** 307–320, 1999.
KLUWER/ESCOM

NMR exchange broadening arising from specific low affinity protein self-association: Analysis of nitrogen-15 nuclear relaxation for rat CD2 domain 1

Mark Pfuhl[a], Ho A. Chen[a], Søren M. Kristensen[b] & Paul C. Driscoll[a,c,*]
[a]*Department of Biochemistry and Molecular Biology, University College London, Gower Street, London WC1E 6BT, U.K.;* [b]*Department of Chemistry, University of Copenhagen, Universitetsparken 5, DK-2100 København Ø, Denmark;* [c]*Ludwig Institute for Cancer Research, 91 Riding House Street, London W1P 8BT, U.K.*

Received 23 April 1999; Accepted 12 June 1999

Key words: CD2, crystal contacts, exchange broadening, nuclear relaxation, self-association

Abstract

Nuclear spin relaxation monitored by heteronuclear NMR provides a useful method to probe the overall and internal molecular motion for biological macromolecules over a variety of time scales. Nitrogen-15 NMR relaxation parameters have been recorded for the N-terminal domain of the rat T-cell antigen CD2 (CD2d1) in a dilution series from 1.20 mM to 40 μM (pH 6.0, 25 °C). The data have been analysed within the framework of the model-free formalism of Lipari and Szabo to understand the molecular origin of severely enhanced transverse relaxation rates found for certain residues. These data revealed a strong dependence of the derived molecular correlation time τ_c upon the CD2d1 protein concentration. Moreover, a number of amide NH resonances exhibited exchange broadening and chemical shifts both strongly dependent on protein concentration. These amide groups cluster on the major β-sheet surface of CD2d1 that coincides with a major lattice contact in the X-ray structure of the intact ectodomain of rat CD2. The complete set of relaxation data fit well to an equilibrium monomer–dimer exchange model, yielding estimates of exchange rate constants ($k_{ON} = 5000\ M^{-1}\ s^{-1}$; $k_{OFF} = 7\ s^{-1}$) and a dissociation constant ($K_D \sim 3$–6 mM) that is consistent with the difficulty in detecting the weak interactions for this molecule by alternative biophysical methods. The self-association of CD2d1 is essentially invariant to changes in buffer composition and ionic strength and the associated relaxation phenomena cannot be explained as a result of neglecting anisotropic rotational diffusion in the analysis. These observations highlight the necessity to consider low affinity protein self-association interactions as a source of residue specific exchange phenomena in NMR spectra of macromolecular biomolecules, before the assignment of more elaborate intramolecular conformational mechanisms.

Introduction

The use of heteronuclear ^{15}N and ^{13}C nuclear relaxation measurements is a generally accepted tool for the analysis of biomolecular dynamics over a broad range of timescales ranging from picoseconds to seconds (Peng and Wagner, 1992; Lane and Lefèvre, 1995; Dayie et al., 1996; Jardetzky, 1996; Palmer et al., 1996; Kay, 1998). In the most commonly adopted mode of analysis of such data, namely the 'model-free approach' of Lipari and Szabo (1982a,b) and variants thereof, the most readily accessible derived parameters – including the generalised order parameters S^2 and

*To whom correspondence should be addressed. E-mail: driscoll@biochem.ucl.ac.uk.

Supplementary material: Lists of residue-specific R_1, R_2 and NOE values for CD2d1 in 10 mM phosphate buffer, pH 6.0, and concentrations of 40 μM, 0.1, 0.2, 0.4, 0.8 and 1.2 mM as well as at [CD2d1] = 1.2 mM in 10 mM Bis-Tris/HCl, pH 6.0, and in 10 mM phosphate, pH 6.0, with 150 and 300 mM NaCl added can be obtained from the corresponding author, as well as two figures showing the distribution of NH angles with the three principal axes of the inertia tensor of monomeric and dimeric CD2d1.

fast local motion correlation times τ_e – describe the amplitude and timescale of very fast internal vibrational and librational motions. These parameters are of interest to probe fundamental questions concerning protein stability and plasticity (Yang and Kay, 1996). On the other hand, protein function and protein–ligand interactions are often effected by motions on much slower timescales ranging from microseconds to seconds (Lane and Lefèvre, 1995; Jardetzky, 1996; Palmer et al., 1996). In the Lipari–Szabo formalism the evidence of this class of motions emerges only via the introduction of 'exchange' terms (R_{ex}) as correction factors, which are less reliably identified and difficult to interpret (Clore et al., 1990a). The use of spectral density mapping as an alternative mode of analysis (Peng and Wagner, 1992) does not necessarily improve the level of insight, since the excess R_2 relaxation rates are rebranded as contributions to the J(0) spectral density term. Even when exchange contributions to the R_2 relaxation rate are addressed more explicitly, for example with newly developed spectroscopic methods (Szyperski et al., 1993; Akke and Palmer, 1996; Zinn-Justin et al., 1997; Mulder et al., 1998), the interpretation of their physical origin in atomic and mechanistic terms is challenging. Therefore, slow motions detected in heteronuclear relaxation experiments are often attributed to complex conformational rearrangements (LeMaster and Kushlan, 1996; Banci et al., 1998; Volkman et al., 1998). In principle the comparative examination of nuclear relaxation rates and long computer simulations could yield further insights, but at present the limited duration of even the longest dynamics trajectories available, ca. 1 μs (Duan et al., 1998), means that it is difficult to test the veracity of proposed exchange mechanisms.

As part of a long term aim to better understand the basis of protein–protein interactions in immune response (Davis et al., 1998), we have been engaged in the characterisation of the solution behaviour of the N-terminal domain of the rat T-cell adhesion protein CD2 (CD2d1) (Driscoll et al., 1991, 1993; McAlister et al., 1996; Chen et al., 1998). Previously the application of nuclear relaxation analysis for rat CD2d1 in our hands failed to yield consistent values for the fundamental hydrodynamic molecular rotational correlation time parameter (Kieffer and Driscoll, 1992; Crawford, 1994). Following the report of ^{15}N exchange broadening observed for human CD2d1 (Wyss et al., 1997) and serendipitous observation of unusual acidic residue acidity constants (pK_a) in rat CD2d1 (Chen et al., 1999), we have characterised the hydrodynamic and polypeptide dynamics properties of rat CD2d1 using ^{15}N nuclear relaxation measurements over an extensive range of sample conditions. One of the main outcomes of this analysis is confirmation of substantial line broadening for a subset of resonances, in a manner similar to those reported for the homologous human CD2d1 protein (Wyss et al., 1997). In this report we show that the exchange broadening for rat CD2d1 is strongly dependent upon the protein concentration and that the broadened resonances also display considerable concentration-dependent chemical shift variation. These findings, together with the observation of concentration-dependent values of the rotational correlation time τ_c, allow us to identify low affinity self-association of CD2d1 as a major contributory factor in the explanation of its hydrodynamic behaviour. Instances of protein self-association effects as reported in the literature have mainly focused on evaluation of τ_c values (Grzesiek et al., 1997; Fushman et al., 1998; Gryk et al., 1998; Zhang et al., 1998). In contrast, for rat CD2d1 concentration-dependent linewidth effects are observed for the resonances of a specific limited region of the protein surface, which is remarkably coincident with a major intermolecular contact in crystals of the complete extracellular portion (ectodomain) of the CD2 protein (Jones et al., 1992). The data illustrate that residue-specific exchange broadening of ^{15}N NMR resonances can arise from molecular association phenomena, a situation in which the requirement to invoke elaborate mechanisms of conformational change of the polypeptide chain is minimized.

Materials and methods

Sample preparation

Rat CD2d1 protein samples for this study were prepared as described recently (Chen et al., 1998). If not otherwise noted, spectra were recorded using samples containing CD2d1 at concentrations between 40.0 μM and 1.2 mM in 10 mM phosphate buffer. CD2d1 concentrations higher than 1.7 mM tended to cause precipitation and were therefore not used in this study. The solution pH was adjusted by adding small amounts of 1N NaOH or HCl to the final sample. The pH values given are the mean of pH meter readings taken before and after acquisition of the spectrum.

NMR spectroscopy

Spectra were recorded on Varian UnityPlus spectrometers equipped with three radio frequency channels and triple resonance Z-axis pulsed field gradient probes. All the relaxation experiments were measured at a ^{1}H frequency of 500 MHz. The sample temperature was set to 25.0 °C (actual sample temperature, calibrated with ethylene glycol standard). ^{15}N relaxation was studied using standard pulse sequences for ^{15}N R_1 and [^{1}H]-^{15}N heteronuclear NOE (Kay et al., 1989; Barbato et al., 1992). ^{15}N R_2 was measured using a modified sequence to suppress cross-correlation effects of chemical shift anisotropy (CSA) and dipolar interactions (Kay et al., 1992b). The delays used in the CPMG sequence of the R_2 experiment were 0.9 ms. Spectra were acquired with 1024 complex points and a spectral width of 10000 Hz in F2 and 128 complex points, 1600 Hz in F1. The spectra were recorded using States-TPPI (States et al., 1982) phase cycling combined with gradient coherence selection sensitivity enhancement (Palmer et al., 1991; Kay et al., 1992a). Series of 2D spectra were recorded with relaxation time delays of 10.05, 60.29, 130.62, 231.09, 341.62, 482.28, 743.52, 1065.04 and 1507.13 ms for R_1 and 0, 16.87, 33.73, 50.59, 67.45, 84.32, 118.05 and 151.78 ms for R_2 measurements. Recycle delays were 2 s in both R_1 and R_2 experiments. To assess the reproducibility of the spectral intensities the measurement for a relaxation time of 482.28 ms was repeated for the R_1 series and for 33.73 ms in the R_2 series. The heteronuclear NOE was measured with experiments based on polarisation transfer heteronuclear single quantum coherence (HSQC) spectra as reported previously (Barbato et al. 1992). Alternate experiments were measured with and without saturation of protons for a time of 3 s in a total recycle delay of 3.6 s between scans. Each of these two experiments was recorded twice to estimate the reproducibility. Noise levels were estimated from the root mean square (rms) intensities in regions of the spectra void of signals. Complete relaxation data (R_1, R_2, NOE) were obtained for CD2d1 at six different protein concentrations between 1.2 mM and 40 μM. Measurements were started with a sample at 1.2 mM which was subsequently diluted with sample buffer to the target concentration. Protein concentrations were checked at each step by measuring the UV absorption at 280 nm. The number of transients per t_1 increment was increased from 16 at a CD2d1 concentration of 1.2 mM to 128 at a concentration of 40 μM. No NOE measurements were performed at 0.1 mM and 40 μM because of the low inherent sensitivity. NOE values were taken from the measurement at 0.2 mM to perform the complete Lipari–Szabo analysis (there was no detectable trend in the variation of NOE values over the entire concentration range). Control experiments were performed with a sample of rat CD2d1 at a concentration of 1.2 mM in Bis-Tris/HCl buffer (10 mM), pH 6.0, as well as in 10 mM phosphate buffer, pH 6.0, with 150 and 300 mM NaCl, respectively. All spectra were processed with NMRPipe (Delaglio et al., 1995). Free induction decays (FIDs) were multiplied with a Gaussian window function in t_2 with a line broadening of 2.0 Hz and a weighting factor of 0.01 while a squared sine function shifted by 80° was used in t_1. No zero filling was applied in t_2 prior to Fourier transformation while FIDs in t_1 were extended by 32 complex points (from 128 measured to 160) by linear prediction using 8 coefficients followed by zero filling to 512 points prior to Fourier transformation. A second order polynomial baseline correction was performed both in F1 and F2. Spectra were analysed with ANSIG v3.3 (Kraulis, 1989), AZARA (Boucher, 1995) and XEASY (Bartels et al., 1995) . All resonance assignments used in this work are as published (Chen et al., 1998) and can be obtained from the BioMagRes databank, accession number 4109.

Data analysis

Residue-specific ^{15}N relaxation data were analysed according to the Lipari-Szabo model-free formalism (Lipari and Szabo, 1982a,b) with its extension to motions on an intermediate time scale (Clore et al., 1990b) in a manner similar to that described by Palmer and co-workers (Mandel et al., 1995). All numerical analysis was performed in MATHEMATICA (Wolfram, 1988) using the Levenberg–Marquardt method (Wolfram, 1988) for parameter fitting. Estimation of molecular rotational correlation times τ_c was performed along established lines ((Barbato et al., 1992) from the mean value of residue R_2/R_1 ratios using data for a subset of residues not implicated in large-amplitude local motions (resonance selection criteria: $|(|R_2 - \langle R_2\rangle|)/(\langle R_2\rangle) - (|R_1 - \langle R_1\rangle|)/(\langle R_1\rangle)| > 1.5$ SD and heteronuclear NOE > 0.65).

The concentration dependences of apparent (isotropic) rotational correlation times, chemical shift variations and exchange broadening of resonance lines were analysed within the framework of an equilibrium between monomeric CD2d1 (A) and a symmetric CD2d1 homodimer (A_2) according to:

$$A_2 \underset{k_{ON}}{\overset{k_{OFF}}{\rightleftharpoons}} 2 \cdot A \tag{1}$$

$$K_D = \frac{k_{OFF}}{k_{ON}} = \frac{[A_2]}{[A]^2} \tag{2}$$

Over the range of CD2d1 concentrations used, the observed chemical shifts were treated as population-weighted averages of the free monomer and intact dimer values, allowing the extraction of the difference in chemical shifts $\Delta\delta = |\delta(dimer) - \delta(monomer)|$ and a value of the dissociation constant K_D by simple non-linear least square fit of the data for each residue.

The variation in relaxation rates as a function of protein concentration was analysed to extract limiting values for the rotational correlation time of the monomeric CD2d1 at infinite dilution,and the putative intact homodimer CD2d1 at high concentration. In order to perform this estimation, consideration must be given to the appropriate averaging of observables. Since the apparent τ_c is not a linear function of R_1 and R_2 decay rates, or even the R_2/R_1 ratio, the apparent τ_c for a given concentration is not a simple weighted average of the monomer and dimer values. In practice, therefore, the analysis of τ_c as a function of concentration had to be performed by non-linear fit of measured and predicted R_2/R_1 ratios, using τ_c(monomer) and τ_c(dimer) as the variables to be optimized, and with population weighting based upon K_D as a further variable to be optimised as described previously (Grzesiek et al., 1997).

In the case of interconverting monomer and dimer species, the observed R_1 and R_2 decay rates are strictly expected to be biexponential. Fitting of such biexponential decay to the single exponentials usually employed in the analysis of ^{15}N relaxation would be expected to degrade the quality of the fit and lead to bias in favour of the slower relaxation rate. However, in the case of dimerization of molecules below 50 kDa the difference in the relaxation rates is too small to lead to a significant error. Furthermore, as was noted recently (Fushman et al., 1998), often the averaging of the monomer and dimer relaxation occurs on a time scale much faster than the duration of the NMR experiment to measure the relaxation rates. Consequently, nuclear relaxation experiments yield monotonic exponential decays characterised by population weighted average relaxation rates.

Exchange line broadening was estimated according to (Luz and Meiboom, 1963):

$$R_{ex} = (\Delta\omega)^2 \cdot p_A p_{A_2} \cdot k_{ex}^{-1} \cdot \left[1 - \frac{2}{k_{ex}\tau_{CPMG}} \cdot \tanh\left(\frac{k_{ex}\tau_{CPMG}}{2}\right)\right] \tag{3}$$

p_A and p_{A_2} are the mole fractions of monomeric and dimeric CD2, $\Delta\omega$ is the difference in chemical shift for a certain resonance between monomer and dimer and τ_{CPMG} is the CPMG refocusing period used in the R_2 pulse sequence. The values for $p_A p_{A_2}$ as a function of concentration were calculated using the K_D values obtained from the fitting results of chemical shift variation against CD2d1 concentration. Equation 3 was then fit against experimentally derived values of R_{ex} at different concentrations to determine k_{ON}, k_{OFF} and $\Delta\omega$. Exchange rate constants k_{ex} were related to on- and off-rates according to the following equations ([A], concentration of monomer; k_{ON}, rate of association; k_{OFF}, rate of dissociation; τ_{A2}, exchange lifetime of dimer; τ_A, exchange lifetime of monomer):

$$\begin{aligned} k_{ex}^{-1} &= \tau_{ex} = \frac{\tau_A \cdot \tau_{A2}}{\tau_A + \tau_{A2}} \\ \tau_A &= k_{ON}^{-1} \cdot [A]^{-1} \\ \tau_{A2} &= k_{OFF}^{-1} \end{aligned} \tag{4}$$

For Equation 3 the on- and off-rates were introduced through k_{ex} as calculated for each concentration with Equation 4.

As part of the analysis of nuclear relaxation rates, an assessment was made of the impact of anisotropic rotational diffusion upon the profile of derived dynamic parameters. For the rat CD2d1 this check was performed in the following manner. The monomeric model rat CD2d1 structure was derived from residues 1–99 of chain A of the crystal structure of rat CD2 (entry 1HNG in the Protein Data Bank (Jones et al., 1992)). Hydrogen atom coordinates were generated using the HBUILD command of X-PLOR (Brunger, 1993) followed by a 1000 steps of energy minimization in which all heavy atoms were kept fixed. The homodimer model of CD2d1 was taken as the structure represented by the major crystal lattice contact between the N-terminal domains of adjacent CD2 molecules, involving the C′CFG β-sheet faces (Jones et al., 1992). The principal moments of the diffusion tensor for each of the monomer and dimer CD2d1 models were obtained with the program PDBINERTIA (Lee et al., 1997). The model coordinates were then transformed to a Cartesian frame coincident with the directions of the principal axes of the diffusion ten-

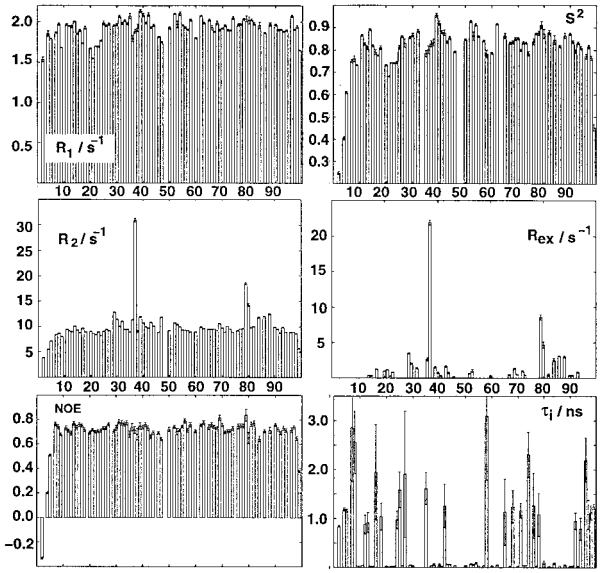

Figure 1. Results of the Lipari–Szabo model free analysis for CD2d1 at 10 mM phosphate buffer, pH 6.0, c = 1.2 mM and T = 25 °C. Left, from top to bottom are ^{15}N relaxation parameters R_1, R_2 and heteronuclear NOE. Right are the major derived parameters of the Lipari–Szabo model-free analysis, from top to bottom S^2, R_{ex} and the local correlation time. Where the simple Lipari–Szabo model was chosen this is τ_e in the ps range. When the extended Lipari–Szabo model had to be employed a very short value for τ_e was assumed and τ_i, which is in the ns range, is displayed. The horizontal scale represents residue numbers.

sor. Angles of NH vectors relative to the principal axis of the diffusion tensor were calculated independently for monomer and dimer models with home written programs. Analysis of relaxation data was limited to the assumption of axially symmetric diffusion as described recently (Tjandra et al., 1995, 1996). The subset of residues used for the analysis was identical to that used in the isotropic analysis. Using the rotational correlation time and $D_{\parallel}/D_{\perp}$ as variable input parameters, calculated values of R_2/R_1, based on a spectral density for overall tumbling extended to incorporate axially symmetric anisotropic rotational diffusion (Woessner, 1962), were fit to the experimentally determined R_2/R_1 ratios. The potential impact of CD2d1 dimerization at higher concentrations was accounted for by fitting residue-specific R_2/R_1 ratios with the population weighted average of anisotropic R_2/R_1 ratios calculated separately for monomer and dimer. This calculation was based on the NH vector angles derived separately for the monomer and dimer diffusion tensor coordinate frames, and the assumption that the rotational correlation time for the intact dimer is twice that of the monomer.

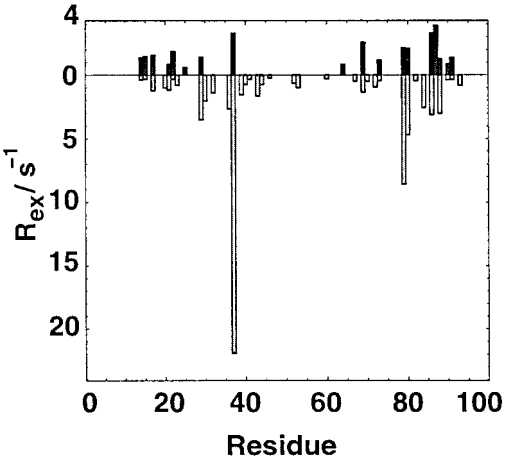

Figure 2. Exchange contribution R_{ex} along the polypeptide chain for rat CD2d1 at 10 mM phosphate buffer, pH = 6.0, T = 25 °C, proton resonance frequency of 500 MHz, protein concentrations of 0.1 mM (black bars) and 1.2 mM (grey bars).

For comparison, rotational diffusion coefficients were also calculated using a bead model as implemented in the program HYDRO (Luz and Meiboom, 1963; de la Torre and Bloomfield, 1981). Amino acids were replaced by spheres of 2.5 Å radius placed on the position of the C_α atoms. Water molecules were replaced by spheres of 1.6 Å radius placed on the position of the oxygen atom. CD2d1 was hydrated by first placing the structural model that was obtained as described above in a box of equilibrated TIP3P water with subsequent removal of those water molecules clashing with atoms in the protein (i.e. within a cutoff distance of 2.3 Å from protein heavy atoms) and energy minimization for 500 steps allowing only water molecules to move and keeping the protein atoms fixed. A hydration shell was created by keeping only a subset of all water molecules from the hydration step within a cutoff distance from protein heavy atoms. Cutoff distances between 2.6 and 3.8 Å were used, leading to hydration shells populated by 78 to 298 water molecules.

Results

Residue-specific relaxation parameters

The ^{15}N relaxation of rat CD2 domain 1 has been characterised over an extensive range of protein concentration and sample conditions. Here the results of a Lipari–Szabo model-free analysis are described in detail for relaxation data obtained with a sample at [CD2d1] = 1.2 mM, pH = 6.0 (10 mM phosphate

buffer), T = 25 °C and 500 MHz proton frequency. An overview of the measured relaxation rates and the results of the model-free analysis is shown in Figure 1. With the exception of the four residues at the N-terminus and the C-terminal residue Glu99, all amino acids in CD2d1 exhibit rather uniform relaxation parameters (average values are $\langle R_1 \rangle = 1.92 \pm 0.08\ s^{-1}$, $\langle R_2 \rangle = 10.00 \pm 1.38\ s^{-1}$ and <heteronuclear NOE> $= 0.71 \pm 0.04$). An apparent molecular rotational correlation time $\tau_c = 7.52 \pm 0.05$ ns is obtained from the average R_2/R_1 ratio for these residues. The results of the model-free analysis are correspondingly uniform with most residues having $S^2 > 0.6$, indicating a fairly rigid overall structure. The mean S^2 of 0.81 ± 0.07 is in accordance with values widely reported in the literature for highly ordered regions of protein structure (Kay et al., 1989). In four short stretches of the polypeptide chain the S^2 values are slightly smaller, with values between 0.6 and 0.8. These regions occur at the long loop connecting β-strands B and C (residues Asn20–Asp25), the loop between strands C and C′ (residues Gly35–Thr37), the loop connecting strand C′ to C″ (residues Lys45–Lys47), and the hairpin turn connecting strands D and E (residues Leu58–Asn60). The derived estimates of the internal motion correlation times are uniformly small (< 50 ps), perhaps indicating fast thermal vibrations. Intermediate-fast timescale dynamics (Clore et al., 1990a) had to be assumed in certain instances, most notably for the first eight residues of the chain. Here the local correlation times have values around 0.8–1.5 ns and the order parameters for the fast timescale motions $S_f^2 \approx 0.7$ (data not shown).

A small number of residues – most notably Thr37 and Thr79 – show very large deviations in the R_2 panel (Figure 1) whilst displaying R_1 and heteronuclear NOE values close to average values. In the Lipari–Szabo analysis these outlier values in the transverse relaxation rate are accounted for by the invocation of exchange contributions to R_2 (for Thr37 $R_{ex} = 22\ s^{-1}$, for Thr79 $R_{ex} = 8\ s^{-1}$). A more detailed view is shown in Figure 1 in the panel displaying the estimated R_{ex} contributions across the polypeptide chain. Here it is apparent that several other residues exhibit smaller but nevertheless significant values of $R_{ex} > 1.5\ s^{-1}$, including Glu29, Val30, Ser36, Val39, Lys43, Val80, Asn84, Thr86 and Leu88.

Effects of protein concentration on residue-specific relaxation parameters

Similar model-free analyses of the relaxation data obtained for CD2d1 at a range of concentrations down to 40 μM were also performed (data not shown). The majority of residue-specific relaxation parameters is not significantly affected by the protein concentration. For most residues, S^2 is greatest at the higher values of protein concentration with slightly lower values estimated from the data at low concentrations. Maximal differences for the S^2 over the concentration range are around ± 0.04, within the order of magnitude of the uncertainty of the derived values. All variations seen for the fast local motions are within the error limits, and the same is true for the time constants for the motions on an intermediate time scale.

The only substantial variations detected in this dilution series are in the profile of R_{ex} exchange contributions to R_2, as shown in Figure 2. The values of R_{ex} in the regions around Glu29–Trp32, Thr37 and Thr79–Thr86 all show a strong dependence on CD2d1 concentration. While these residues exhibit large R_{ex} terms at high protein concentration, these values systematically drop to very small values in the more dilute samples. At the lowest protein concentration studied (40 μM) the relaxation data for a number of those residues with R_{ex} terms at high concentration (e.g. residues Val30, Trp32, Ser36, Val39, Phe42) can be satisfactorily fit without recourse to an exchange contribution. On the other hand, a small number of residues, e.g. Thr69, Thr86 and Leu88 have values of $R_{ex} \sim 2\ s^{-1}$ throughout the dilution series. A representation of the residues which exhibit concentration-dependent R_{ex} terms is indicated in the ribbon diagram (Figure 7) of the domain 1 interaction seen in the crystals of the intact extracellular portion of CD2 (Jones et al., 1992). The disposition of residues which exhibit concentration-dependent R_{ex} terms is consistent with the notion that the exchange terms arise from weak dimerization of the CD2d1 molecule.

The magnitude of R_{ex} terms for Thr37 ($22\ s^{-1}$) and Thr79 ($8\ s^{-1}$) is exceptionally large, outside the range that could be accounted for by neglect or underestimation of rotational diffusion anisotropy, and very strongly dependent of protein concentration. The concentration dependence of the exchange broadening for these residues is presented in Figure 3. A reasonably good fit for the R_{ex} values is obtained within a monomer–dimer equilibrium model using Equations 3 and 4. The value of K_D necessary to calculate the fractional amounts of monomer and dimer in Equation 3 is

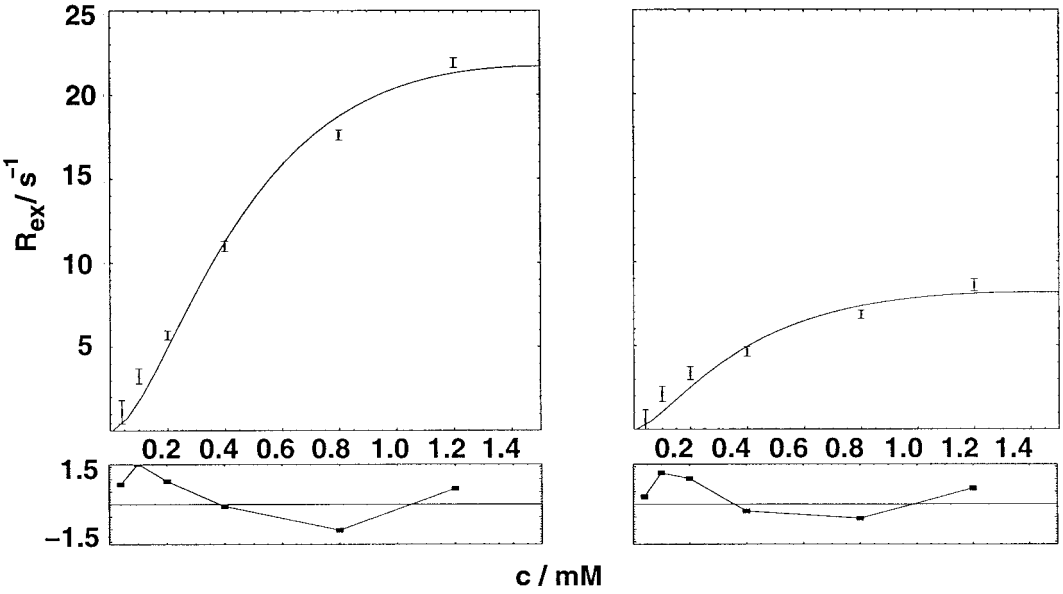

Figure 3. Variation of ^{15}N line-broadening as a function of protein concentration for Thr37 (left) and Thr79 (right) at 10 mM phosphate buffer, pH = 6.0 and T = 25 °C. The upper panels show the experimental data plus a curve obtained from fitting the data to the function defined by Equation 3. The lower panels display the residuals from the fit.

taken from the fit of the chemical shift vs. concentration of the corresponding residue (see below). These estimated values of K_D are also used to relate k_{ON} and k_{OFF} according to Equation 2. This reduces the number of parameters that are optimised in the fitting procedure to $\Delta\omega$ and k_{ON}, the latter in the form of τ_{ex} through Equation 4. From the curve fit for the data for Thr37 we obtained values for $\Delta\omega/2\pi = 130 \pm 5$ Hz ($\sim$ 2.6 ppm), $k_{ON} = 4200 \pm 600$ M^{-1} s^{-1} and $k_{OFF} = 9 \pm 2$ s^{-1}. The corresponding fit for Thr79 yielded $\Delta\omega/2\pi$ = 79 $\pm$ 6 Hz ($\sim$ 1.6 ppm), $k_{ON} = 4500 \pm 1200$ M^{-1} s^{-1} and $k_{OFF} = 5 \pm 2$ s^{-1}.

Concentration dependence of chemical shifts

Chemical shifts in ^{15}N-^{1}H HSQC spectra of CD2d1 were monitored over a protein concentration range from 1.2 mM to 40 μM. Extreme caution was taken to maintain stable sample buffer conditions (concentration and pH) over the dilution range. A small number of residues demonstrated significant ^{15}N chemical shift variation of up to 0.5 ppm over this range. The majority of these residues were amongst those which exhibit considerable exchange broadening at the higher concentrations of CD2 (see above). Residues with the largest values in chemical shift variation cluster in two regions of the polypeptide chain, around positions 28–46 and 78–90. Chemical shift versus protein concentration plots are illustrated in Figure 4 for the two residues with the largest variation, Thr37 and Thr79. Curve fitting to a monomer–dimer equilibrium as described by Equation 3 yields extrapolated CD2d1 dimer–monomer chemical shift differences of $\Delta\delta = 1.97 \pm 0.11$ ppm for Thr37 and $\Delta\delta = 1.12 \pm 0.2$ ppm for Thr79. These values are in good agreement with the values extracted from the fitting of the concentration of dependence of R_{ex} terms which are $\Delta\delta = 2.6$ ppm for Thr37 and 1.6 ppm for Thr79, respectively. Dissociation constant K_D values estimated from the curve fitting are 4.6 ± 1.8 mM and 5.4 ± 2.2 mM for Thr37 and Thr79, respectively.

Isotropic rotational diffusion of CD2d1

The apparent rotational correlation time of CD2d1 was found to depend strongly on the protein concentration. The variation of τ_c with protein concentration, obtained from independent analysis of relaxation data sets for each dilution of the sample, is shown in Figure 5. A substantial influence of the protein concentration over the range from 40 μM to 1.2 mM upon the derived value of τ_c is seen, covering an interval of approximately 2 ns. The variation in experimental τ_c values was then fit to a monomer–dimer equilibrium model using Equation 1, as shown in Figure 5, yielding extrapolated values for CD2d1 monomer and dimer τ_c of 5.02 $\pm$ 0.1 ns and 10.09 $\pm$ 0.5 ns re-

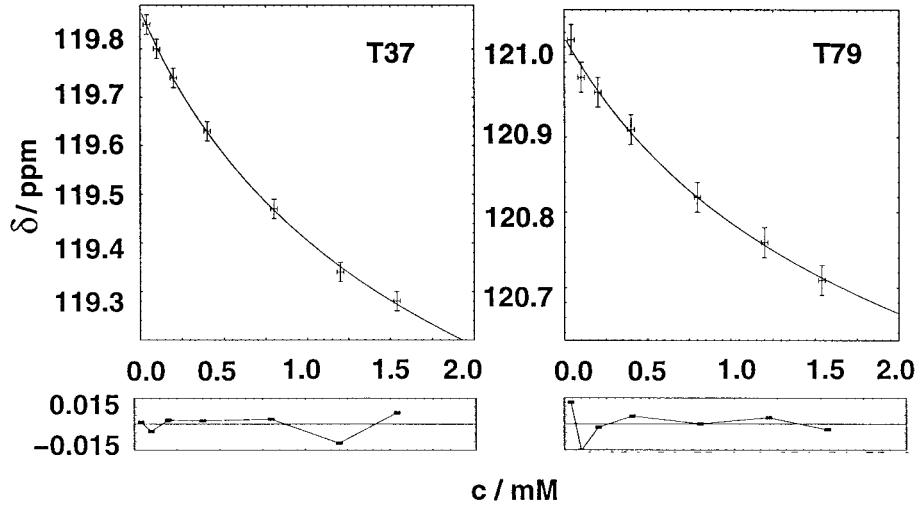

Figure 4. Variation of ^{15}N chemical shifts as a function of CD2d1 concentration for Thr37 and Thr79 at 10 mM phosphate buffer, pH = 6.0 and T = 25 °C. The upper panels show the experimental data plus a curve obtained from a fit to a function representing the chemical shift as a population average of monomer and dimer values. The lower panels display the residuals from the fit.

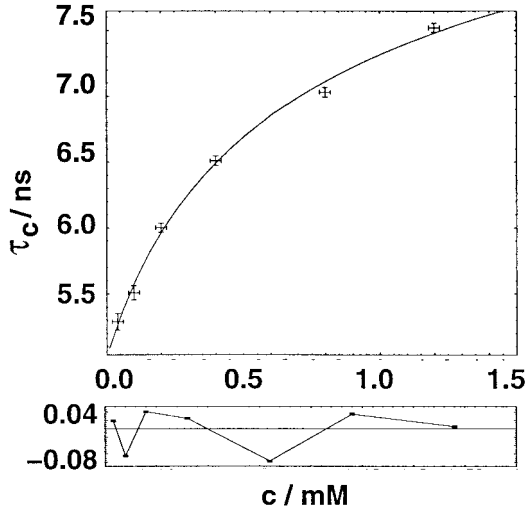

Figure 5. Dependence of the apparent rotational correlation time τ_c of rat CD2d1 on protein concentration at 10 mM phosphate buffer, pH = 6.0 and T = 25 °C. The upper panel shows the fit of τ_c to a monomer-dimer equilibrium (using Equation 1) assuming population averaged τ_c values. The lower panel shows the residuals of the fit.

spectively. The value of the dissociation constant K_D obtained in this fit was found to be 2.6 ± 0.7 mM.

Further measurements of CD2d1 τ_c were performed in different buffers and salt concentrations to exclude spurious solvent or specific ion effects as a source for the observed dynamics phenomena (see Table 1). The value of τ_c was measured at three values of the ionic strength: a sample of 1.2 mM CD2d1 in 10 mM phosphate buffer, pH 6.0, and the same sample with 150 mM NaCl and 300 mM NaCl added, respectively. Also shown in Table 1 is the result of a measurement for 1.2 mM CD2d1 in 10 mM Bis-Tris/HCl buffer, pH 6.0. The variation of τ_c amongst all conditions for the high concentration is only marginally greater than the measurement error.

Table 1. Dependence of rotational correlation time of CD2d1 and ^{15}N exchange line broadening of Thr37 on buffer conditions at pH = 6.0, protein concentration of 1.2 mM, T = 25 °C

Buffer condition	τ_c /(ns)	Thr37 R_{ex} /(s^{-1})
10 mM phosphate	7.52 ± 0.04	21.9 ± 0.3
10 mM phosphate, 150 mM NaCl	7.67 ± 0.05	27.1 ± 0.8
10 mM phosphate, 300 mM NaCl	7.71 ± 0.06	24.1 ± 2.0
10 mM Bis-Tris/HCl	7.81 ± 0.05	23.2 ± 0.2

Anisotropic rotational diffusion of CD2d1

Calculation of the principal axes of the inertia tensor for the monomer and homodimer (derived from the major crystal contact) models for CD2d1 using a bead model (de la Torre and Bloomfield, 1981; de la Torre et al., 1994) indicates approximately cylindrical shapes of the monomer as well as the dimer. The monomer model therefore predicts axially symmetric tumbling with values of $D_\parallel/D_\perp = 1.41$ for unhydrated CD2d1 and values between 1.34 and 1.39 for hydrated CD2d1, independent of the cutoff distance

for hydration (between 2.4 and 3.8 Å, corresponding to between 14 and 297 molecules of water). Essentially identical $D_{\parallel}/D_{\perp}$ values (hydrated $D_{\parallel}/D_{\perp} = 1.35$ and unhydrated $D_{\parallel}/D_{\perp} = 1.42$) were obtained for the homodimeric models of CD2d1. However, the orientation of the principal axis system with respect to the molecular coordinates is different in the monomer and dimer models of CD2d1. Therefore, for a given residue the angle made by the NH vector to the principal axis is considerably different in each case. Analysis within the framework of axially symmetric anisotropic rotational diffusion was performed for the experimental ^{15}N relaxation data measured for CD2d1 at concentrations of 0.1 mM and 1.2 mM. At [CD2d1] = 0.1 mM it was assumed that dimeric CD2d1 would give only a marginal contribution to the measured data (assuming a K_D around 2–4 mM gives only $\sim$ 5% dimer at [CD2d1] = 0.1 mM). The $D_{\parallel}/D_{\perp}$ ratio derived from fitting the relaxation data was found to be $D_{\parallel}/D_{\perp} = 1.39 \pm 0.15$, with the 95% confidence interval ranging from 1.01 to 1.71. The improvement in the χ^2 value of this fit compared with the fit to an isotropic model is only modest ($\chi^2_{aniso} = 145.2$; $\chi^2_{iso} = 171.2$). Consequently, according to an F-statistic, this improvement in the fit is not significant ($F = 4.02$, $p = 0.104$). To be considered statistically significant, values of $F \gg 5$ and $p \ll 0.01$ are usually required.

The relaxation data at [CD2d1] = 1.2 mM were analysed under the assumption of a significant contribution of the dimer to the measured data (at 1.2 mM and assuming a K_D around 2–4 mM there will be at least $\sim$ 30% dimer present). A value for $D_{\parallel}/D_{\perp} = 1.50 \pm 0.21$ with a 95% confidence interval from 1.1 to 1.71 was obtained for the monomer and $D_{\parallel}/D_{\perp} = 1.20 \pm 0.11$ with a 95% confidence interval from 0.9 to 1.41 for the dimer. However, the result of the fitting to an anisotropic model again compared poorly to the result from the isotropic model ($\chi^2_{aniso} = 1908.1$ and $\chi^2_{iso} = 2221.4$). The reduction of the χ^2 value leads to $F = 1.77$ and $p = 0.11$, also not sufficient to be considered statistically significant.

Effects of salt and buffer on residue-specific relaxation parameters

Consistent with the behaviour of τ_c, only small variations were seen on the residue-specific level with alteration of buffer and salt content. Order parameters S^2 were largest in the sample without added salt and dropped only slightly (by about 0.04) above 150 mM NaCl (data not shown). However, these changes were small and within the margin of experimental uncertainty for the majority of residues. Larger changes in the values of S^2 (around 0.06) were seen only for the highly mobile N-terminal three residues. Internal motion correlation times were uniformly smaller than 80 ps for fast motions and between 1.0 and 4.0 ns for intermediate time scale motions. No consistent trend of the dependence of internal motion correlation time values τ_i on the salt concentration could be identified. The pattern of residues with substantial R_{ex} terms is essentially unaffected by changes in ionic strength as shown in Figure 6. For most residues between Glu29–Lys47 and Asn77–Ile88 there is a slight increase in R_{ex} values at 300 mM NaCl. Three residues (Lys45, Lys47, Thr83) exhibit more elevated values of $R_{ex} > 5\ s^{-1}$. The residue-specific relaxation parameters measured in Bis-Tris/HCl buffer are identical within the error margin to those measured in phosphate buffer at similar pH, buffer and protein concentrations (data not shown).

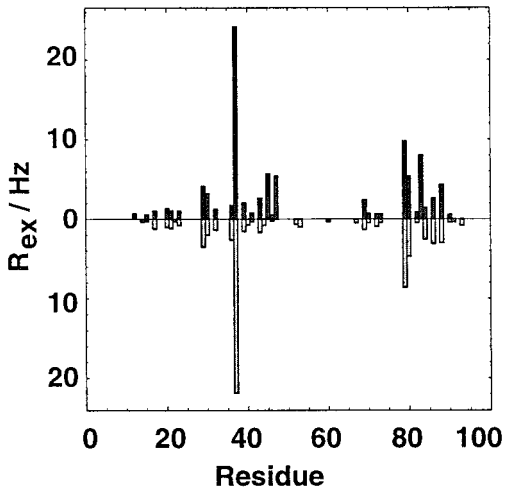

Figure 6. Exchange contribution R_{ex} along the polypeptide chain of rat CD2d1 at 10 mM phosphate buffer, pH = 6.0, T = 25 °C and a proton resonance frequency of 500 MHz for samples with 0 (grey bars) and 300 mM added NaCl (black bars).

Discussion

Line broadening and CD2d1 dimerization

Our measurements unambiguously demonstrate that the very fast ^{15}N transverse relaxation rates observed for some residues in CD2d1, interpreted as a result of specific exchange broadening, depend on the protein concentration (see Figures 2 and 3). The fact

that only few residues are affected and that all of these show a weak but detectable concentration dependence of their ^{15}N chemical shifts (Figure 4) rules out bulk solvent properties, such as variation in macroscopic sample viscosity, as a cause. The observed effects are also remarkably stable to changes in ionic strength and type of buffer in the sample. Further support for low-affinity CD2d1 self-association as the cause for the unusual resonance line broadening is derived from the observation that all concentration-dependent NMR parameters can be fit reasonably well to the homodimerization model with a K_D of the order of 3–6 mM. The distribution of residues that exhibit ^{15}N exchange broadening is illustrated in Figure 7. The structure shown includes the major CD2d1 interprotein crystal contact which comprises the apposition of the C′CFG β-sheet surfaces together with pairwise reciprocal backbone-backbone H-bond formation between the C-C′ loop (residues Arg34–Leu38) in one monomer with the F-G loop (residues Val80–Asn84) in the other. The residues with large R_{ex} terms cluster in the interfacial region of the crystal contact. The crystal contact excludes some 600–700 Å^2 of surface area for each rat CD2 molecule and has attracted attention as a model for the analogous physiological interaction of CD2 with its homologous adhesion partners (CD48 in rat, CD58 in human) (Jones et al., 1992). For residues Thr37 and Thr79 in particular, the magnitudes of the R_{ex} values are so great that they cannot be accounted for by the neglect or underestimation of the rotational diffusion anisotropy (Tjandra et al., 1995), anomalous variation in NH bond length, or ^{15}N CSA tensor magnitude or orientation (Fushman et al., 1998). Attempts to detect self-association of CD2 in solution by a range of biophysical techniques have so far failed (van der Merwe, 1993; Silkowski et al., 1997). However, the relaxation data reported here clearly suggest that CD2d1 self-association, albeit of low affinity, does take place at millimolar concentrations.

Analysis of CD2d1 rotational diffusion

Because it has been illustrated that inappropriate interpretation of ^{15}N R_{ex} terms may arise from failure to take into account anisotropic rotational diffusion (Tjandra et al., 1995, 1996) we sought to analyse the CD2d1 relaxation data within such a framework. Analysis of structural models for monomeric and dimeric CD2d1 exhibits considerable degrees of anisotropy in the principal components of their inertia tensors with $D_\parallel/D_\perp$ for both monomer and dimer $\approx$ 1.4. Our NMR-derived experimental values of $D_\parallel/D_\perp \sim 1.5 \pm 0.2$ for [CD2d1] = 0.1 mM and $D_\parallel/D_\perp$ (monomer) $\sim 1.2 \pm 0.1/D_\parallel/D_\perp$ (dimer) $\sim 1.5 \pm 0.1$ for [CD2d1] = 1.2 mM match quite well the predictions based on bead models. This good correspondence of the experimental data to the expectation is, however, undermined by the lack of statistical significance in the result. There appear to be two main reasons for poor reliability of the anisotropy estimates: the limited precision of the relaxation data, and poor angular sampling of the diffusion tensor by the set of NH bond vectors (Lee et al., 1997). The latter observation seems of particular relevance in the case of monomeric CD2d1 since more than 1/3 of the residues have angles of their NH vectors to the main axis of the inertia tensor between 80–100°, with another 15 each between 60–80° and 100–120°, making it more than 70% of all residues in a narrow region of angles (see supplementary material for more details). The majority of residues is thus expected to exhibit similar R_2/R_1 ratios, leaving only a few residues to provide more divergent values. The result of fitting such an uneven distribution of R_2/R_1 ratios might therefore produce a meaningful result but not in a statistical significant manner. An additional reason for a lack of detectable CD2d1 anisotropy at [CD2d1] = 1.2 mM is found in the substantial difference of angles that the NH vectors make with the principal axes of the inertia tensor in each of the monomer and dimer states. In a sample that contains comparable amounts of both monomer and dimer the ^{15}N nucleus of a given residue will relax according to an averaged combination of different values of R_2/R_1. With a large difference in the orientation of the principal axes of the inertia tensor in monomer and dimer structures (in the case of the CD2d1 models this is about 80°), large values of R_2/R_1 will be automatically combined with small values, resulting in an averaging out of the effects of diffusion anisotropy. Only in situations where the principal axes of the inertia tensor coincide for monomer and dimer will it be possible to reliably detect anisotropic diffusion in an equilibrium between monomer and dimer states.

In the absence of statistically significant diffusion anisotropy of CD2d1 we have analysed the variation of derived isotropic relaxation parameters in terms of a fast exchange dimerization equilibrium for CD2d1. The isotropic τ_c values for monomeric and dimeric CD2d1 extrapolated from the curve fit shown in Figure 5 are in good agreement with values calculated from the simple Stokes– Einstein relationship (including a fractional hydration of 0.32 and assuming that

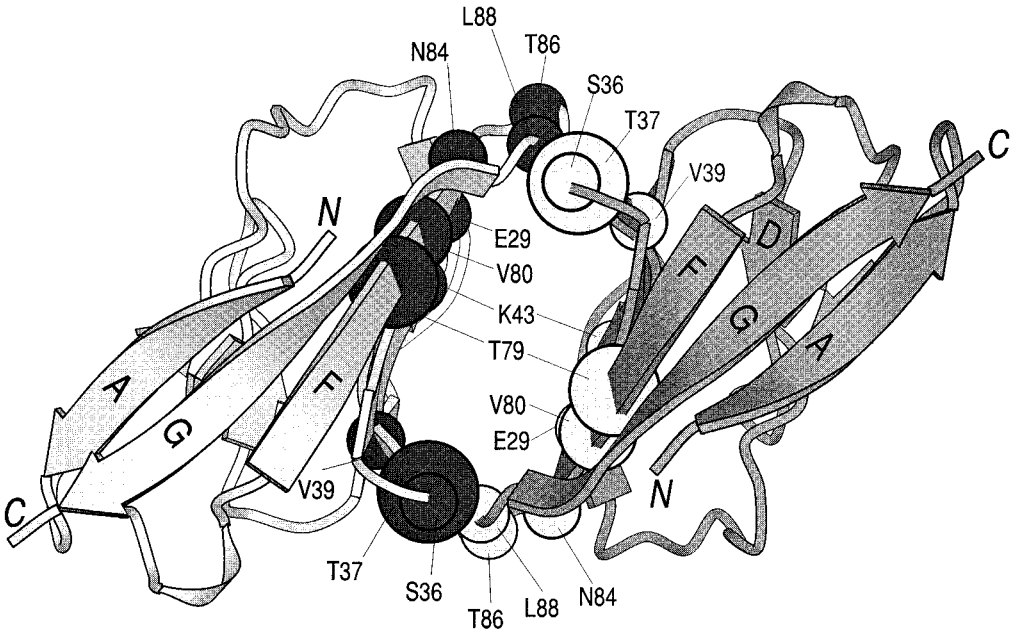

Figure 7. CD2d1 dimer interface as seen in the rat CD2 crystal structure. For clarity the two monomers are shaded in different degrees of grey. Residues with $R_{ex} > 1.5\ s^{-1}$ are marked by a sphere centred on the position of the corresponding backbone nitrogen. The radius of the sphere is approximately proportional to the magnitude of R_{ex}.

the total molecular mass – including hydration – of the dimer is twice that of the monomer). An excellent agreement is obtained of the measured values of 5.02 $\pm$ 0.1 and 10.09 $\pm$ 0.5 ns with the theoretical values of 4.9 and 9.8 ns for monomer and dimer, respectively.

The values for the dissociation constant K_D obtained from fitting τ_c (2.6 $\pm$ 0.7 mM) and chemical shift (average for Thr37 and Thr79 K_D = 5.0 $\pm$ 2.0 mM) vs. concentration profiles are in good agreement. However, it should be noted that the precision of K_D measurements by any method is generally low (Weber, 1992), as also indicated here by the much larger fitting error for K_D than for the maximal chemical shift difference or τ_c values. The average on- and off-rates extracted from fitting R_{ex} values for two residues Thr37 and Thr79 ($k_{ON} \approx 5000\ M^{-1}\ s^{-1}$ and $k_{OFF} \approx 7\ s^{-1}$) compare well within the considerable error to the kinetic constants measured for the analogous physiological high affinity CD2-CD48 interaction (Davis et al., 1998) $k_{ON} = 10^5\ M^{-1}\ s^{-1}$, $k_{OFF} = 8\ s^{-1}$. It appears that the lower affinity for CD2d1 self-association is mainly a result of a substantially reduced k_{ON} rate constant.

Thr37 and Thr79 chemical shift variation

Chemical shift differences for the two threonines were obtained with good agreement from the analysis of concentration-dependent chemical shift and R_{ex} values, indicating that the mechanism behind both is identical and essentially driven by dimerisation. The substantial chemical shift variations with protein concentration (Figure 4) must therefore result from changes in the nuclear shielding between the monomer and dimer states of CD2d1. It is noteworthy that for Thr37 and Thr79 there is an absence of a comparable variation of the associated H^N proton resonance frequency (data not shown). Recent theoretical considerations of the nature of amide ^{15}N shielding parameters suggest that the major influences arise from hydrogen bond formation, both by the NH group itself and by the carbonyl group of the preceding amino acid residue (Le and Oldfield, 1996), the polypeptide backbone conformation (Le and Oldfield, 1994), metal ion coordination by the carbonyl group (Biekofsky et al., 1998) and the γ-gauche effects of the χ_1 angle in β-branched amino acids (Le and Oldfield, 1996; Biekofsky et al., 1998). The increased shielding of the Thr37 and Thr79 ^{15}N chemical shifts at higher CD2d1 concentration and the lack of a strong perturbation of the H^N chemical shifts indicate that the hydrogen bonding influence on the shift variation is not dominant. In the CD2 crystal structure the Thr79 NH and Val78 CO groups make only intra-monomer antiparallel β-sheet H-bonds. The Thr37 NH makes

an intra-monomer H-bond with Arg34 CO in the C-C′ loop. The Ser36 CO group makes an inter-molecular H-bond with Arg87 of the opposing CD2 molecule and therefore might be expected to give rise to a deshielding effect for the Thr37 ^{15}N resonance upon dimerization. However, the upfield trend in the ^{15}N chemical shifts (see Figure 4) with increasing CD2d1 concentration is opposite to that predicted for the creation or strengthening of H-bonds. Instead it is likely that the ^{15}N chemical shifts for these two residues are more strongly affected by alterations in the γ-gauche shielding effects from the β-branched threonine side chain that would accompany changes in the χ_1 side chain torsion angle upon dimerization.

Comparison of rat and human CD2d1 dynamics

Wagner and co-workers have previously reported a detailed study of the ^{15}N relaxation properties of the homologous human CD2d1 domain (Wyss et al., 1997). To facilitate comparison with our results on rat CD2d1 the raw relaxation data for human CD2d1, originally interpreted using the spectral-density mapping approach (Peng and Wagner, 1992; Wyss et al., 1997), were re-analysed within the model-free formalism (data not shown). Under similar solution conditions (human CD2d1 relaxation data were measured on a $\sim$ 1 mM protein sample in 20 mM acetate at pH = 4.5; rat CD2d1 1.2 mM protein concentration, 10 mM phosphate buffer at pH = 6.0; temperature = 25 °C in both cases), a very similar dynamic behaviour is seen for both proteins. The overall tumbling time of human CD2d1 (τ_c = 8.8 ns) compares well with the value (τ_c = 7.52 ns) obtained for rat CD2d1 since human CD2d1 has a slightly longer polypeptide chain and an N-linked glycan attached. Both proteins have essentially identical average order parameters and the regions of the polypeptide chain with slightly lower order parameters superimpose almost perfectly (particularly in the extended loop connecting the B-C strands of the β-sheet). Most interestingly, similarly large R_{ex} values are found in human CD2d1 for some residues in the ligand-binding interface (Phe47 17 s^{-1}; Glu50 11 s^{-1}; Thr53 16 s^{-1}) very close in the sequence and structure alignment to Thr37 and Thr79 (22 s^{-1} and 8 s^{-1}, respectively) in rat CD2d1. Crystals of human CD2 possess a major crystal contact that is topologically identical to that observed for rat CD2, in spite of significant sequence differences between the contact surfaces of the two proteins (Bodian et al., 1994). All residues affected by ^{15}N exchange broadening in both proteins are clustered, albeit in slightly different arrangements, on this self-association surface.

Conclusions

We have demonstrated a strong correlation of protein self-association and residue-specific exchange line broadening as measured using ^{15}N relaxation data of rat CD2d1. This result demonstrates that protein self-association has sizeable effects at the typical concentrations used in NMR experiments. Even very low affinity interactions, perhaps beyond the limit that can be detected by other methods, should therefore not be ignored in the interpretation of nuclear relaxation data (Akke et al., 1998). It should also be pointed out that because of the factor $p_A p_{A_2}$ in Equation 3 a maximal effect of dimerization on exchange broadening is already achieved at concentrations well below K_D (the exchange broadening coefficient $p_A p_{A_2}$ has a maximum of 0.25 for $p_A = p_{A_2} = 0.5$). Moreover, the effects of self-association need not appear as a non-specific effect (Fushman et al., 1998; Gryk et al., 1998) but rather can give rise to indications of localised and residue-specific exchange broadening. This conclusion may prove to be of general significance in efforts to ascribe specific conformational mechanisms for exchange phenomena. In a few cases, very detailed descriptions have been given for well-defined conformational rearrangements, such as isomerisation of disulfide bonds (Otting et al., 1993; LeMaster and Kushlan, 1996) and the backbone peptide bond of proline residues (Evans et al., 1989). In general, this type of conformational change results in resolution of distinct resonances in slow exchange. In other cases rather unspecific descriptions of the movement of surface loops or flexing of secondary structure elements are linked to the exchange phenomena (Wong et al., 1997; Akke et al., 1998; Banci et al., 1998; Volkman et al., 1998). Since surface loops and extended surfaces of β-sheets and α-helices are candidate regions for exchange broadening from both protein self-association as well as true intramolecular conformational changes, it may be desirable to obtain a more detailed description of the molecular details of such movements. For example the attribution of exchange broadening of ^{15}N resonances in the C′CFG β-sheet of human CD2d1 to flexibility of the β-sheet (Wyss et al., 1997) may warrant further examination.

As the most simple precaution to avoid misinterpretation of exchange terms in the study of protein

dynamics, nuclear relaxation measurements should preferably include a dilution series. In only a few previously reported cases has there been explicit consideration of the effects of self-association upon nuclear relaxation rates (Grzesiek et al., 1997; Akke et al., 1998; Fushman et al., 1998), and rarely has this included deliberate measurements of relaxation rates over a range of concentrations. In principle self-association can be detected by careful monitoring of chemical shifts as a function of protein concentration. However, very great care is required to maintain identical sample conditions over the dilution as other influences upon chemical shifts can be dominant. For example for CD2d1 pH dependent changes of the chemical shifts are pervasive in the pH 5.0–7.0 range (Chen et al., 1998). Self-association of proteins targeted for NMR study is undesirable for a variety of reasons and it is noteworthy that the effects observed in the case of CD2d1 were not significantly affected by the addition of salt and the use of a different buffer, which are commonly adopted remedies of problems with sample conditions in biomolecular NMR spectroscopy. In cases where it might be suspected that the interaction is of biological significance it will be beneficial to perform relaxation experiments at least at high and low concentrations to determine accurate values of τ_c to quantify the oligomerisation state. A full characterisation of the kinetics involved in exchange processes will require a more complete analysis of the relaxation rates over a range of protein concentration as we have shown here for CD2d1. An additional benefit of such a strategy would be the acquisition of low concentration estimates of τ_c to facilitate a more accurate correlation of protein molecular weight, shape factors and hydration with experimental hydrodynamic parameters. Thereby the large deviations of calculated from measured values of τ_c, recently compiled in a study comparing molecular weight and accessible surface area (Krishnan and Cosman, 1998), might be considerably improved.

Acknowledgements

During the course of this work P.C.D. was a Royal Society University Research fellow, and M.P. a long-term EMBO postdoctoral fellow. The authors wish to thank Dr. F. Delaglio for provision of the NMRPipe data processing software, Drs. A.G. Palmer and N. Tjandra for making available their computer programs for the analysis of anisotropic rotational diffusion, and Professor G. Wagner for providing the relaxation data for human CD2d1.

References

Akke, M. and Palmer, A.G. (1996) *J. Am. Chem. Soc.*, **118**, 911–912.
Akke, M., Liu, J., Cavanagh, J., Erickson, H.P. and Palmer, A.G. (1998) *Nat. Struct. Biol.*, **5**, 55–59.
Banci, L., Felli, I. and Koulougliotis, D. (1998) *J. Biomol. NMR*, **12**, 307-318.
Barbato, G., Ikura, M., Kay, L. E., Pastor, R. W. and Bax, A. (1992) *Biochemistry*, **31**, 5269–5278.
Bartels, C., Xia, T.-H., Billeter, M., Güntert, P. and Wüthrich, K. (1995) *J. Biomol. NMR*, **6**, 1–10.
Biekofsky, R.R., Martin, S.R., Browne, J.P., Bayley, P.M. and Feeney, J. (1998) *Biochemistry*, **37**, 7617–7629.
Bodian, D.L., Jones, E.Y., Harlos, K., Stuart, D.I., and Davis, S.J. (1994) *Structure*, **2**, 755–766.
Boucher, W. (1995) *AZARA v1.0, Department of Biochemistry, University of Cambridge, U.K.*
Brunger, A.T. (1993) *XPLOR*.v.31, Yale University, New Haven, CT.
Chen, H.A., Pfuhl, M., Davis, B. and Driscoll, P.C. (1998) *J. Biomol. NMR*, **12**, 457–458.
Chen, H.A., Pfuhl, M., McAlister, M. S.B. and Driscoll, P.C. (1999) submitted.
Clore, G.M., Driscoll, P.C., Wingfield, P.T. and Gronenborn, A.M. (1990) *Biochemistry*, **29**, 7387.
Clore, G.M., Szabo, A., Bax, A., Kay, L.E., Driscoll, P.C. and Gronenborn, A.M. (1990) *J. Am. Chem. Soc.*, **112**, 4989–4991.
Crawford, D.A. (1994) *Structure and Dynamics of a Cell Adhesion Protein*, Ph.D. Thesis, Oxford University, Oxford.
Davis, S.J., Ikemizu, S., Wild, M.K. and van der Merwe, P.A. (1998) *Immunol. Rev.*, **163**, 217–236.
Dayie, K.T., Wagner, G. and Lefèvre, J.F., In *Dynamics and the Problem of Recognition in Biological Macromolecules*, Nato ASI Series A, Vol. 288, Plenum Press, New York, NY, pp. 139–162.
de la Torre, J.G. and Bloomfield, V.A. (1981) *Q. Rev. Biophys.*, **14**, 81–139.
de la Torre, J.G., Navarro, S., Martinez, M.C.L., Diaz, F.G. and Cascales, J.J.L. (1994) *Biophys. J.*, **67**, 530–531.
Delaglio, F., Gzesiek, S., Vuister, G.W., Zhu, G., Pfeifer, J. and Bax, A. (1995) *J. Biomol. NMR*, **6**, 277–293.
Driscoll, P.C., Cyster, J.G., Campbell, I.D. and Williams, A.F. (1991) *Nature*, **353**, 762–765.
Driscoll, P.C., Cyster, J.G., Somoza, C., Crawford, D.A., Howe, P., Harvey, T.S., Kieffer, B., Campbell, I.D. and Williams, A.F. (1993) *Biochem. Soc. Trans.*, **21**, 947–952.
Duan, Y., Wang, L. and Kollman, P.A. (1998) *Proc. Natl. Acad. Sci. USA*, **95**, 9897–9902.
Evans, P.A., Kautz, R.A., Fox, R.O. and Dobson, C.M. (1989) *Biochemistry*, **28**, 362–370.
Fushman, D., Cahill, S. and Cowburn, D. (1998) *J. Mol. Biol.*, **266**, 173–194.
Gryk, M.R., Abseher, R., Simon, B., Nilges, M. and Oschkinat, H. (1998) *J. Mol. Biol.*, **280**, 879–896.
Grzesiek, S., Bax, A., Hu, J.-S., Kaufman, J., Palmer, I., Stahl, S.J., Tjandra, N. and Wingfield, P. (1997) *Protein Sci.*, **6**, 1248–1261.
Jardetzky, O. (1996) *Prog. Biophys. Mol. Biol.*, **65**, 171–218.
Jones, E.Y., Davis, S.J., Williams, A.F., Harlos, K. and Stuart, D.I. (1992) *Nature*, **360**, 232–239.

Kay, L.E. (1998) *Nat. Struct. Biol.*, **5**, 513–517.
Kay, L.E., Torchia, D.A. and Bax, A. (1989) *Biochemistry*, **28**, 8972–8979.
Kay, L.E., Keifer, P. and Saarinen, T. (1992) *J. Am. Chem. Soc.*, **114**, 10663.
Kay, L.E., Nicholson, L.K., Delaglio, F., Bax, A. and Torchia, D.A. (1992) *J. Magn. Reson.*, **97**, 359–367.
Kieffer, B. and Driscoll, P.C. (1992) unpublished observations.
Kraulis, P.J. (1989) *J. Magn. Reson.*, **24**, 627–633.
Krishnan, V.V. and Cosman, M. (1998) *J. Biomol. NMR*, **12**, 177–182.
Lane, A.N. and Lefèvre, J.-F. (1995) *Methods Enzymol.*, **239**, 596–619.
Le, H. and Oldfield, E. (1994) *J. Biomol. NMR*, **4**, 341–348.
Le, H.B. and Oldfield, E. (1996) *J. Phys. Chem.*, **100**, 16423–16428.
Lee, L.K., Rance, M., Chazin, W.J. and Palmer, A.G. (1997) *J. Biomol. NMR*, **9**, 287–298.
LeMaster, D.M. and Kushlan, D.M. (1996) *J. Am. Chem. Soc.*, **118**, 9255–9264.
Lipari, G. and Szabo, A. (1982a) *J. Am. Chem. Soc.*, **104**, 4546–4559.
Lipari, G. and Szabo, A. (1982b) *J. Am. Chem. Soc.*, **104**, 4559–4570.
Luz, Z. and Meiboom, S. (1963) *J. Chem. Phys.*, **39**, 366–370.
Mandel, A.M., Akke, M. and Palmer, A.G. (1995) *J. Mol. Biol.*, **246**, 144–163.
McAlister, M.S.B., Mott, H.R., van der Merwe, P.A., Campbell, I.D., Davis, S.J. and Driscoll, P.C. (1996) *Biochemistry*, **35**, 5982–5991.
Mulder, F.A.A., de Graaf, R.A., Kaptein, R. and Boelens, R. (1998) *J. Magn. Reson.*, **131**, 351–357.
Otting, G., Liepinsh, E. and Wüthrich, K. (1993) *Biochemistry*, **32**, 3571–3582.
Palmer, A.G., Cavanagh, J., Wright, P.E. and Rance, M. (1991) *J. Magn. Reson.*, **93**, 151–170.
Palmer, A.G., Williams, J. and McDermott, A. (1996) *J. Phys. Chem.*, **100**, 13293–13310.
Peng, J.W. and Wagner, G. (1992) *J. Magn. Reson.*, **98**, 308–332.
Silkowski, H., Davis, S.J., Barcley, A.N., Rowe, A.J., Harding, S.E. and Byron, O. (1997) *Eur. Biophys. J.*, **25**, 455–462.
States, D.J., Haberkorn, R.A. and Ruben, D.J. (1982) *J. Magn. Reson.*, **48**, 286–292.
Szyperski, T., Luginbühl, P., Otting, G. and Wüthrich, K. (1993) *J. Biomol. NMR*, **3**, 151–164.
Tjandra, N., Feller, S.E., Pastor, R.W. and Bax, A. (1995) *J. Am. Chem. Soc.*, **117**, 12562–12566.
Tjandra, N., Wingfield, P., Stahl, S. and Bax, A. (1996) *J. Biomol. NMR*, **8**, 273–284.
van der Merwe, P.A. (1993) personal communication.
Volkman, B.F., Alam, S.L., Satterlee, J.D. and Markley, J.L. (1998) *Biochemistry*, **37**, 10906–10919.
Weber, G. (1992) *Protein Interactions*, Chapman and Hall, New York, NY.
Woessner, D.E. (1962) *J. Chem. Phys.*, **37**, 647–654.
Wolfram, S. (1998) *Mathematica–A System for Doing Mathematics by Computer*, 2.0 edition, Wolfram Research Inc., Champaign, IL.
Wong, K.-B., Fersht, A.R. and Freund, S.M.V. (1997) *J. Mol. Biol.*, **258**, 494–511.
Wyss, D.F., Dayie, K.T. and Wagner, G. (1997) *Protein Sci.*, **6**, 534–542.
Yang, D. and Kay, L.E. (1996) *J. Mol. Biol.*, **263**, 369–382.
Zhang, W.X., Smithgall, T.E. and Gmeiner, W.H. (1998) *Biochemistry*, **37**, 7119–7126.
Zinn-Justin, S., Berthault, P., Guenneugues, M. and Desvaux, H. (1997) *J. Biomol. NMR*, **10**, 363–372.